BOLETÍN GEOLÓGICO Y MINERO
2022, VOL. 133 (2), 45-63
ISSN: 0366-0176
http://dx.doi.org/10.21701/bolgeomin/133.2/002

Boletín Geológico y Minero

RESEARCH ARTICLE

Geochemical and isotopic study of phreatic aquifer in an arid area, case study of El Golea region (Algerian Sahara)

Estudio geoquímico e isotópico de un acuífero freático en una zona árida. Caso de estudio en la región de El Golea (Sahara argelino)

Bilal Fenazi[1], Aziez Zeddouri[1], Fatih Boucenna[2]

[1] Laboratoire des Réservoirs Souterrains Pétroliers, Gaziers et Aquifères, Faculté des Hydrocarbures, des Energies Renouvelables et des Sciences de la Terre et de l'Univers, Université Kasdi Merbah, Route de Ghardaïa, BP. 511, 30000, Ouargla, Argelia
[2] Centre Universitaire de Tamanrasset, Route de l'Aéroport. BP. 10034, 11000, Tamanrasset, Argelia

Corresponding author: b_fenazi@yahoo.fr (Bilal Fenazi)

Key points

There is a strong correlation between electrical conductivity and the majority of chemical elements

Carbonate minerals (calcite) are oversaturated in all groundwater samples

Isotopic composition depletion can be explained by the presence of mixes of phreatic groundwater and Continental Intercalaire

ABSTRACT

Shallow groundwater is a major reservoir of water in arid areas. This water is characterized by strong mineralization which represents a major quality problem for human consumption and even for its use in agriculture. For this reason, geochemical, statistical and isotopic studies were conducted to obtain an overview of the processes that control water mineralization in the oasis of El Golea (Algerian Sahara). Spatial distributions of EC in this area show that the highest concentrations are situated close to the El Golea Lake formed by evaporitic rock. Geochemical and statistical analysis and data from 28 water points in the phreatic aquifer of the El Golea oasis show a strong correlation between electrical conductivity and the majority of chemical elements, indicating the influence of the interaction between fresh water and bed rock on this mineralization. The results obtained indicate that Carbonate minerals (calcite) are oversaturated in all groundwater samples. The ionic ratios demonstrate the role of weathering, dissolving, ion exchange, and evaporation procedures in mineralization acquisition. The scatter plot of that relates $\delta^2H = f(\delta^{18}O)$ reveals that all of the samples were founds to be below both the GMWL of Craig (1961) and the Sfax local meteoric boundaries (South Tunisia) indicating that groundwater samples have an old origin. This isotopic composition depletion can be explained by the presence of mixes of phreatic groundwater and Continental Intercalaire (CI) (W2).

Keywords: Arid zones; El Golea; Geochemistry; Isotope; Mineralization.

Article History:
Received: 24/04/2020
Accepted: 24/12/2021

Puntos clave

Existe una correlación elevada entre la conductividad eléctrica y la mayoría de los elementos químicos

Los minerales de carbonato (calcita) están sobresaturados en todas las muestras de agua subterránea

La composición isotópica puede explicarse por la presencia de mezclas de agua subterránea freática y Continental Intercalaire

RESUMEN

El agua subterránea poco profunda es un importante depósito de agua en las zonas áridas. Esta agua se caracteriza por una elevada mineralización que representa un gran problema de calidad para el consumo humano e incluso para su uso en agricultura. Por este motivo, se realizaron estudios geoquímicos, estadísticos e isotópicos para obtener una visión general de los procesos que controlan la mineralización del agua en el oasis de El Golea (Sahara argelino). Las distribuciones espaciales de CE en esta área muestran que las concentraciones más altas se encuentran cerca del lago El Golea formado por materiales evaporíticos. El análisis geoquímico y estadístico y los datos de 28 puntos de agua en el acuífero freático del oasis de El Golea muestran una correlación elevada entre la conductividad eléctrica y la mayoría de los elementos químicos, lo que indica la influencia en esta mineralizaciónde la interacción entre el agua dulce y el material acuífero. Los resultados obtenidos indican que los minerales de carbonato (calcita) están sobresaturados en todas las muestras de agua subterránea. Las proporciones iónicas demuestran el papel de los procesos de meteorización, disolución, intercambio iónico y evaporaciónen la adquisición de mineralización. El gráfico de dispersión que relaciona $\delta 2H = f(\delta^{18}O)$ revela que se encontró que todas las muestras estaban por debajo del GMWL de Craig (1961) y los límites meteóricos locales de Sfax (sur de Túnez), lo que indica que las muestras de agua subterránea tienen un origen antiguo. Este agotamiento de la composición isotópica puede explicarse por la presencia de mezclas de agua subterránea freática y Continental Intercalaire (CI) (W2).

Palabras clave: Zonas áridas; El Golea; Geoquímica; Isótopos; Mineralización.

Historial del artículo:
Recibido: 24/04/2020
Aceptado: 24/12/2021

1. Introduction

Water is a scarce and precious resource and it's an indispensable element for human life (Nascimento, 2017). It also contributes to economic development and to maintain ecosystems (Kendra *et al*., 2010; Observatoire Régionale de l'Environnement, 2015). In some cases, this resource becomes a source of covetousness and sometimes of conflict (Ministry of the Environment, 2002). Approximately 41% of the world's land surface is occupied by arid areas (Mortimore, 2009). This arid area is characterized by climatic stress where potential evapotranspiration exceeds rainfall (Yang *et al*., 2011; FIDA, 2016). Due to the scarcity of rainfall, governments have come to use groundwater as the only source capable of satisfying the different sectors of use (Saadé-Sbeih and Jaubert, 2012; Bougharriou *et al*., 2018).

Groundwater bodies most threatened by the degradation of their quality are the shallow (phreatic) ones (Benajiba *et al*., 2013; Knouz *et al*., 2016). This degradation can be explained by the increase in population which requires a relatively high rate of extraction, thus causing pollution generated by anthropogenic activities (Raj and Shaji, 2017; Yang *et al*., 2016).

The oasis of El Golea, in the south of Algeria, is an arid region of the Algerian Sahara that contains two aquifers. The first one phreatic with over-mineralized water, and the other deep with a low rate of mineralization (Continental Intercalaire CI). The high mineralization of the phreatic aquifer that characterizes arid areas seems to be responsible for water quality deterioration and the reduction of agricultural land yields (Zeddouri *et al*., 2010; Kloppmann *et al*., 2011). The variation in groundwater mineralization is mainly a function of the relationship between water facies and the mineralogical composition of the reservoir rock (dissolution and precipitation of minerals), evaporation, oxidation-reduction, transformation of organic matter and anthropogenic activities (Al-Khashman *et al*., 2011; Pazand *et al*., 2018; Allia *et al*., 2018).

This study aims at identifying the hydrochemical processes of groundwater mineralization in the shallow aquifer in the El Golea oasis. The geochemical and statistical approach represents the most suitable technique to characterize the chemical variation of water. This approach has been used by several researchers (BenAmmar *et al*., 2014; Bouteldjaoui *et al*., 2016; Kabour and Chebbah, 2017; Gouaidia *et al*., 2018; Amrani and Hinaje, 2019; Melouah and Zerrouki, 2020). The combination of multivariate statistical approaches such as Principal Component Analysis (PCA) and Hierarchical Cluster Analysis (HCA) is a powerful tool for determining hydrochemical characteristics that influence water geochemistry (Alberto and Del Pilar, 2001; Bouteraa *et al*., 2019), and to identify certain anomalies such as the anthropogenic effect (impact of agricultural activity) on the chemical composition of water (Pereira *et al*., 2003; Bouteraa *et al*., 2019). The basic hydrochemical analysis as well as water facies, ionic ratio and saturation indices (SI) is used to know the factors controlling groundwater geochemistry of the samples in the study area (Zaidi *et al*., 2017). The isotopic study of some samples of this aquifer (phreatic aquifer) aims at indicating the origin and the mechanisms of groundwater recharge.

2. Description of the study area

The study area is situated in a saharian region of Ghardaia district. El Golea is an oasis formed on the bed of the Seggueur Wadi with a surface area of 50km^2, located between 30°22'13" to 30°38'31"N latitude and 2°51'56" to 2°56'04"E longitude. It is bounded by Ghardaïa to the north, Ain Salah to the south, Ouargla to the east and Timimoun to the west (Figure 1).

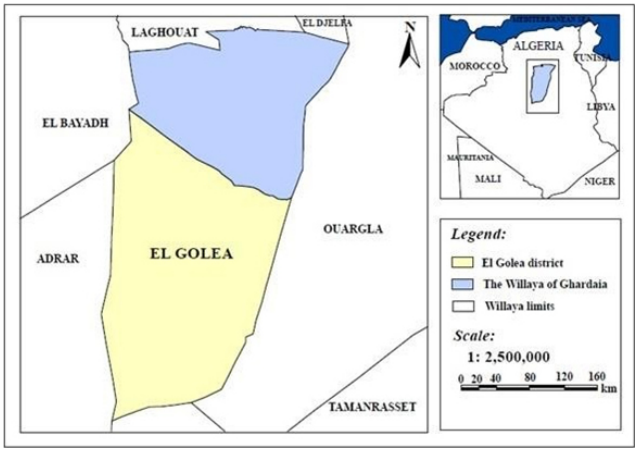

Figure 1. Location of the study area.

Figura 1. Localización del área de estudio.

The oasis of El Golea has a very arid Saharan climate, with a cold winter (8 °C) and a hot and dry summer (36 °C); rainfall is rare and irregular. In 2009, for example, the value of annual precip-

itation was 20 mm, while in 2011 it did not exceed 3.4 mm. Potential evaporation rates is estimated at 2200 mm/year due to the aridity that characterizes this oasis (Dubost, 1992). The study area contains three main units: the first located in the north where the agricultural farmland occupies this part; in the center of the region, an urban area where wastewater flows directly or in to the phreatic aquifer. The raison of that is because most of the population uses septic tanks. There is also a channel where the outlet is the lake. The third part located to the south of the region represented mainly by the lake (Figure 2).

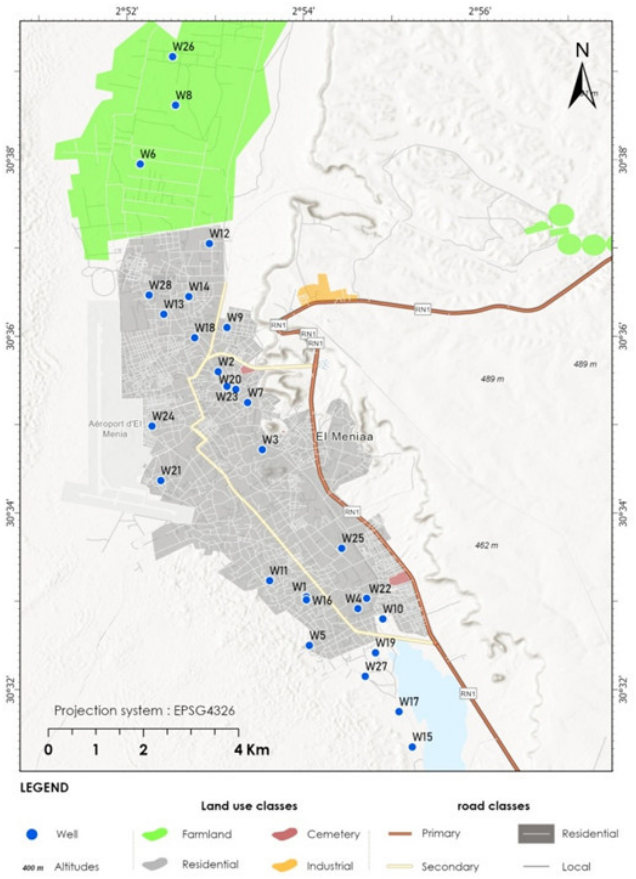

Figure 2. Soil of the study area.

Figura 2. Los suelos del área de estudio.

3. Geology and hydrogeology

The maximum elevation is 400 m above mean sea level on the northeastern side of the area of study, and the minimum elevation is around 360 m on the southern side (the lake). Generally, the ground surface slopes towards southeast direction (Figure 8).

The geology of the El Golea region represented essentially by three types of deposits (Figure 3) characteristic of the desert environment (Peron, 1883):

a. Limestone crust of Turonian age, which is found mainly on the three limestone plateaus at El Golea;
b. Wadi alluvium composed almost exclusively of sandstone (carbonate cement) with clayey levels developed especially in the valley of the Seggueur Wadi;
c. Dunes of the Western Erg totally covering the Cretaceous substratum towards the west, covering very large sectors.

From a hydrogeological point of view, it seems that the study area consists of two aquifers and a lake.

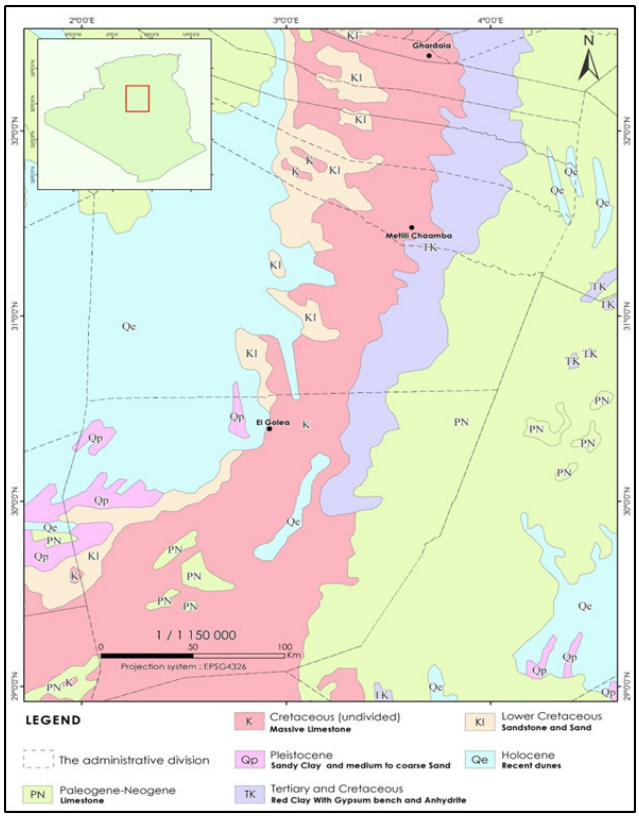

Figure 3. Geological map of the study area (Busson, 1972).

Figura 3. Mapa geológico de la zona de estudio (Busson, 1972).

3.1. Phreatic aquifer

According to Gouskov (1952), the aquifer is essentially composed of alluvial deposits (sandstone) with carbonate cement (Figure 4). The depth of the groundwater varies between 0.65 cm and 1.7 m. This aquifer is supplied by water from

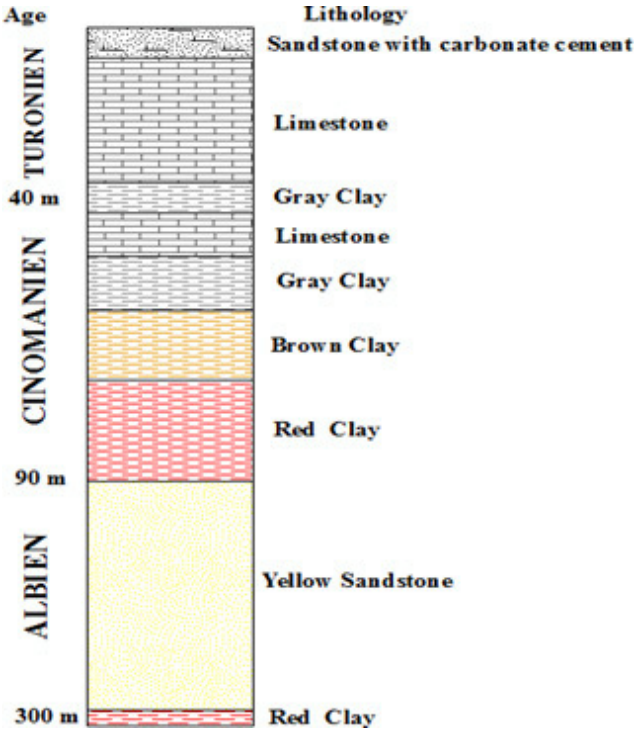

Figure 4. Lithostratigraphy of the study area.

Figura 4. Litoestratigrafía del área de estudio.

Seggueur Wadi during the downpours that often affect this area either by the infiltration of excess of water irrigation. The thickness of this aquifer is between 10 to 12m. The number of water level measures of November 2018 and the distribution of wells in the space was adequate to permit the elaboration of water level contour lines by Ordinary Kriging (Figure 5). Water levels varied from more than 395 to less than 378 m above mean sea level (Table 1), outlining a direction of groundwater flow from the recharge areas (irrigated fields) located in the northwest towards the lake of El Golea, situated in the south.

3.2. Continental Intercalaire aquifer

The CI aquifer is one of the largest confined aquifers in the world formed by a continental formations of the Lower Cretaceous (Neocomian, Barremian, Aptian, Albian) (Moulla *et al.*, 2012) and covers some 600 000 km^2 with a potential reservoir thickness between 120 and 1000 m (Castany, 1982; Hamed *et al.*, 2014), this aquifer continuous west to east from the Guir-Saoura valley to the Libyan desert and north to south from the Saharan Atlas to the Tassili Oua N'Ahaggar divided into two sub-basins (Occidental and Oriental) by the M'zab dorsal (N-S direction) (Cornet, 1964; UNESCO, 1972; Guendouz, 1985).

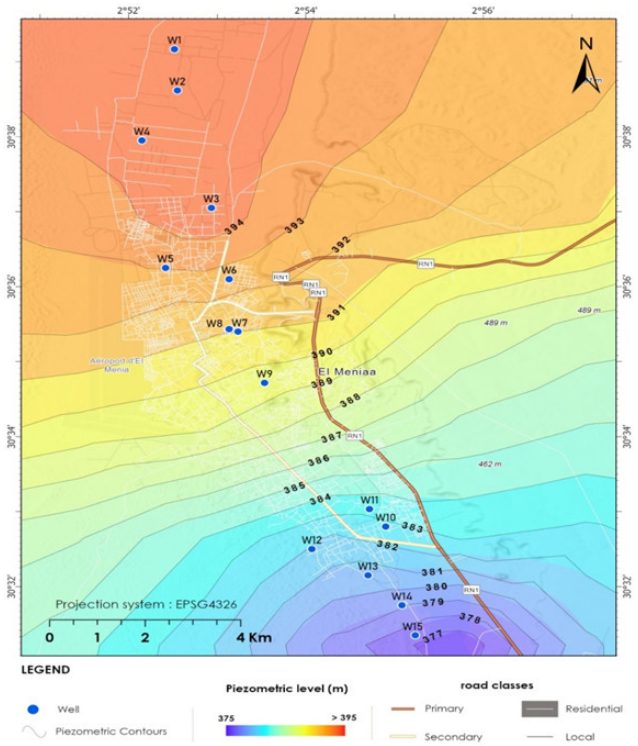

Figure 5. Water level contours line of November 2018.

Figura 5. Líneas isopiezas de Noviembre de 2018.

Wells	Elevation head (Z) (m)	Static head (m)	Piezometric head (m)	Use	Position
W1	397.4	-1.7	395.7	Irrigation	Away from septic tanks
W2	397	-1.7	395.3	Irrigation	Away from septic tanks
W3	395.9	-1.4	394.5	Irrigation	Away from septic tanks
W4	396.2	-1.5	394.7	Irrigation	Away from septic tanks
W5	394.4	-1.2	393.2	Irrigation	Near from septic tanks
W6	393.9	-1.2	392.7	Irrigation	Near from septic tanks
W7	391.9	-0.9	391	Irrigation	Near from septic tanks
W8	392.2	-1	391.2	Irrigation	Near from septic tanks
W9	390.5	-0.9	389.6	Irrigation	Near from septic tanks
W10	382.6	-0.5	382.10	Irrigation	Near from septic tanks
W11	384	-0.7	383.3	Irrigation	Near from septic tanks
W12	382.45	-0.5	381.95	Irrigation	Near from septic tanks
W13	381.15	-0.4	380.75	Irrigation	Near from the lake
W14	379.5	-0.35	379.15	Irrigation	Near from the lake
W15	377.65	-0.25	377.4	Irrigation	Near from the lake

Table 1. Variations of static and piezometric head in the phreatic aquifer.

Tabla 1. Isopiezas y evolución piezométrica en el acuífero freático.

Three processes can be controlled the recharge of this aquifer:

– Run-off at the borders, in the north by the wadi beds at the piedmont (foothills) of the

Saharan Atlas and in the east by the M'zab dorsal
- Run-off at the plateaus borders (Tademaït plateau)
- Rare and torrential rainfall whose rapidly infiltrates the sand dunes (characteristic of arid semi-arid area)

According to Hakimi *et al.* (2021), the EC increases along the W-E direction (Figure 6). The $\delta^{18}O$ isotope ratios in the CI groundwater presents homogenous values and range from -7.5 to -8.5 ‰ and are indicative of Late Pleistocene recharge (Moulla *et al.*, 2012) and the age of this CI groundwater ranges between 20 000 and 40000 years (Moulla, 2005). Table 2 presents the Electric conductivity and isotopic data for 15 water points of CI groundwater (El Golea area).

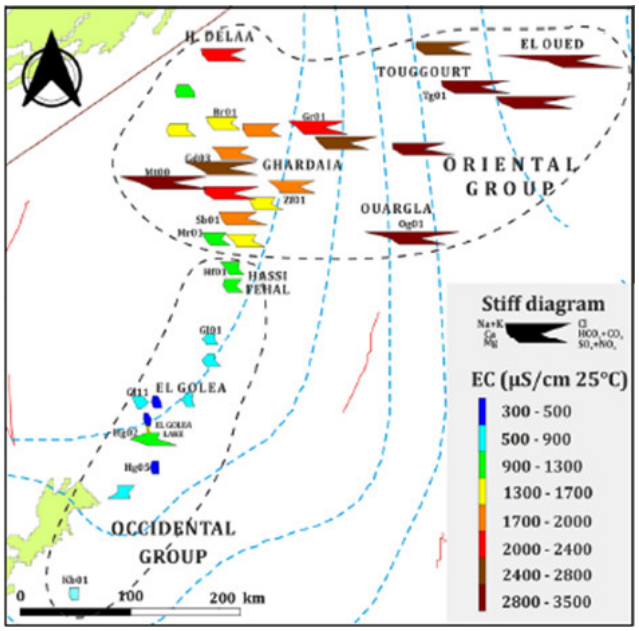

Figure 6. Spatial evolution of physical parameters and chemical water type of the CI groundwater (Hakimi *et al.*, 2021).

Figura 6. Evolución espacial de los parámetros físicos y de la facies del agua subterránea del CI (Hakimi *et al.*, 2021).

3.3. El Golea salt lake

El Golea salt lake is a salt marsh with a surface of 0.19 km² for a maximum depth of 2.5 m, located in the northern Sahara (El-Yamine *et al.*, 2018), bordered on one side by El Golea oasis and on the other side by natural border (rocky hills and sand dunes) (Hacene *et al.*, 2004). The bottom of this lake is composed of evaporitic rock (Guerradi, 2012).

Wells	EC (µS/cm)	$\delta^{18}O$ (‰)	$\delta^{2}H$ (‰)
F1	291	-7.5	-63.3
F2	505	-6.7	-58.7
F3	511	-4.3	-49.7
F4	450	-5.8	-53.4
F5	593	-7.22	-58.2
F6	334	-7.34	-56.25
F7	348	-7.99	-62.07
F8	523	-7.44	-56.03
F9	531	-7.48	-56.89
F10	384	-7.25	-58.63
F11	443	-7.03	-57.67
F12	472	-6.72	-56.26
F13	468	-6.33	-59.54
F14	508	-5.93	-58.31
F15	288	-8.12	-68.96

Table 2. Electric conductivity and isotopic data for 15 water points of CI groundwater (El Golea area).

Tabla 2. Conductividad eléctrica y datos isotópicos de 15 puntos de agua subterránea del CI (área de El Golea).

Figure 7 represents a diagram of the conceptual hydrogeological model of the study area with the relationship between the phreatic, the CI aquifers and finally the lake of El Golea.

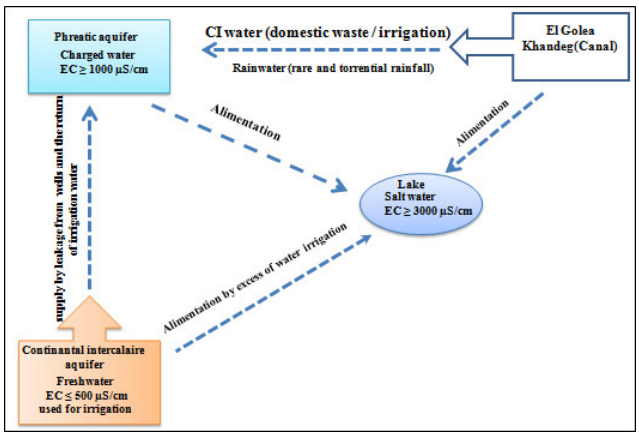

Figure 7. Diagram of conceptual hydrogeological model of the study area.

Figura 7. Diagrama del modelo hidrogeológico conceptual del área de estudio.

The El Golea canal (Khandeg) is intended to evacuate the excess of irrigation water and the waste water results from the exploitation of the CI groundwater (the main resource currently exploited) and phreatic groundwater (low flow compared with CI flow). The lake of El Golea represents a natural outlet of the phreatic aquifer and the canal (Khandeg).

4. Methods and materials

4.1. Sampling analysis

Water samples were taken in four campaigns between November 2015 and November 2018. 28 water points covering the study area were analyzed (Figure 8). In cold storage, these samples were collected in bottles of 500 mL polyethylene (2 to 4°C). In situ measurements of EC (accuracy of ± 0.5% of measured value) and pH (accuracy of ± 0.01 pH units) were performed with a conductivity meter and a WTW 330i pH meter. The major ions (Na^+, Mg^{2+}, Ca^{2+}, K^+, Cl^-, SO_4^{2-}, HCO_3^- and NO_3^-) were evaluated using high performance ion liquid chromatography (HPILC) with IC / Pak TM CM / D columns for cations using EDTA and nitric acid as eluent. We used a Metrohm chromatograph with CI SUPER-SEP columns for anions and phthalic acid and acetonitrile as eluent. The ions total detection limit was 0.04 mg/L. Titration with 0.1N HCl was used in the laboratory to determine HCO_3^- concentrations. For all samples, the ion balance error was less than 5%.

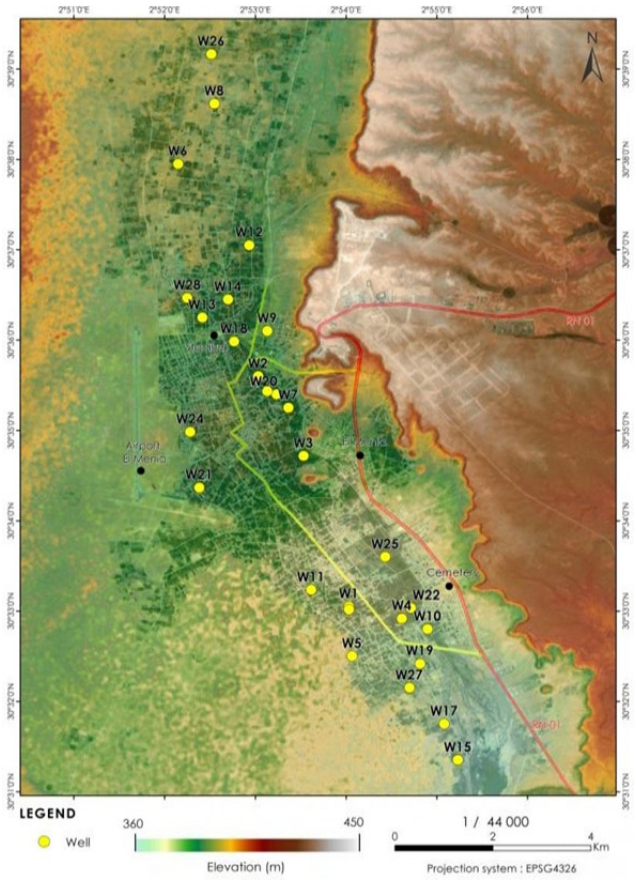

Figure 8. Location of sampling wells.

Figura 8. Localización de los pozos muestreados.

For isotope analyses, six groundwater samples were analyzed for stable isotopes (^{18}O and ^{2}H) using the LGR DLT 100 laser absorption spectrometer (Penna *et al.*, 2010). The results were reported relative to the V-SMOW (Vienna-Standard Mean Oceanic Water) standard. The analytical precisions of $\delta^{18}O$ and $\delta^{2}H$ were ±0.2‰ and ±1.0‰, respectively (Table 7). All of these investigations were carried out at the National School of Engineers Sfax's Radio-Analysis and Environment Laboratory (Tunisia).

4.2. Statistical analysis

A bivariate statistical method used to describe the relationship between hydrochemical ions is correlation analysis of groundwater quality measures. A high correlation coefficient (near to -1 or 1) indicates that two variables have a good link. Values close to 0 indicate that they have no relationship.

In the field of water geochemistry, several scientists have used statistical methods such as Principal Component Analysis (PCA) and Hierarchical Cluster Analysis (HCA) to classify waters and to determine their origin (Belkhiri *et al.*, 2010; Varol *et al.*, 2012; Salman *et al.*, 2015; Boughariou *et al.*, 2018; Bouteraa *et al.*, 2019). These tools are very effective given the case of exploring multivariate data holding multiple variables. PCA is the most widely used method (Farnham *et al.*, 2003; Boughariou *et al.*, 2018) because of the simplicity of its algebra and its direct interpretation. It can be considered as a projection method that projects observations from a p-dimensional space with p variables to a k-dimensional space (where k < p) to retain the maximum amount of information. In this study, the information was measured by the total variance of the scatter plots with respect to the initial dimensions (Paul *et al.*, 2013). Given the existing correlation in the base line data, factor loadings are responsible for the correlations between the main components and the selected variables, with those with the largest positive and negative charges make the largest contribution (Karimipour *et al.*, 2005; Olsen *et al.*, 2012; Sappa *et al.*, 2014; Boughariou *et al.*, 2018).

The varimax rotation was performed on the main components to facilitate the interpretation of the factors according to the natural or anthropogenic processes that control water mineralization. Within the framework of this study, PCA was performed on all 28 groundwater samples from El Golea. It was performed on reduced centered varia-

bles using the Statistica 13.4.0 software package. Ten variables, namely physicochemical parameters (pH and EC) and major ions (Ca^{2+}, Mg^{2+}, Na^{+}, K^{+}, Cl^{-}, HCO_3^{-}, SO_4^{2-} and NO_3^{-}) were considered.

The most powerful grouping mechanism for genetically classifying samples is HCA, a multivariate statistical technique applied in this work (Li *et al*., 2013; Subba Rao *et al*., 2013; Subba Rao and Maya Chaudhary, 2019). Ward's approach was used to perform the Q-mode HCA method on the normalized data set, utilizing Euclidean distance as the measure of similarity. A short Euclidean distance indicates that the measured variables are quite similar. Dendrogram is a graphical depiction of hierarchical clustering or grouping and the corresponding distance to achieve a linkage. The HCA clusters and groups were employed for a more thorough interpretation of the chemical data in terms of 10 chemical variables (pH, EC, Ca^{2+}, Mg^{2+}, Na^{+}, K^{+}, HCO_3^{-}, Cl^{-}, SO_4^{2-} and NO_3^{-}) and 28 groundwater samples.

4.3. Geochemical modeling

Geochemical modeling was assessed with basic geochemical tools including the assessment of raw data, the Piper diagram (Piper, 1953), the determination of major ion ratio, the saturation index (SI) and**,** finally**,** the study of stable isotope ($\delta^{18}O$ and $\delta^{2}H$ ratio).

To supply an insight to groundwater composition, we combined raw data results with hydrogeological information and land use activities. We use ions ratio (in meq/L) to have an overview of the processes that control groundwater characteristics (Subramani *et al*., 2010; Voutsis *et al*., 2015). In this study, the ratio of (Ca^{2+}/Mg^{2+}) vs samples number; Ca^{2+} vs HCO3- ; Na^{+} vs Cl^{-}; ($Ca^{2+} + Mg^{2+}$) vs Cl^{-} were used to study weathering and dissolution process; ($Ca^{2+} + Mg^{2+}$) vs (HCO3- + SO42-) to study ions exchange process and (Na^{+}/Cl^{-}) vs EC to study evaporation process (Krishnaraj *et al*., 2011; Tziritis *et al*., 2016).

A saturation index (SI) using analytical data can be calculated to determine the equilibrium state of the water with respect to a mineral phase (Garrels and Mackenzie, 1967). To identify which geochemical reactions are important in controlling water chemistry, the observation of changes in saturation state can be useful (Coetsiers and Walraevens, 2006; Aghazadeh *et al*., 2016). The SI of a mineral is obtained from Eq.1 (Garrels and Mackenzie, 1967).

$$IS=Log(IAP)/K \quad (1)$$

IAP is the ion activity product of the dissociated chemical species in solution, and K signifies the equilibrium solubility. The saturation indices were calculated using the PHREEQC for Windows hydrogeochemical equilibrium model (Parkhurst and Appelo, 1999).

The value of this index may be zero in the case where the water is saturated by the mineral in question, positive in the case of oversaturation, and negative in the case of undersaturation with respect to this mineral.

In the early1950's, isotopes began to be applied as an important diagnostic tool in groundwater studies (Farid *et al*., 2015). In water isotope, light water molecules have a higher zero point energy than heavy water molecules, needing less energy to slight phase from liquid vapour. As a result, the water molecule with the lowest energy barrier for phase change will preferentially evaporate during evaporation, resulting in residual water that gets increasingly heavier or enriched in $\delta^{18}O$ and $\delta^{2}H$. Heavy isotopes of water, on the other hand are the first to fall as rain, resulting in water vapor masses that grow lighter as one advances inland from a water source or to a higher elevation (Krishnaraj *et al*., 2011). The study of isotopes present in water allows determining the origin of different water masses, to understand the mechanism of acquisition of water salinity and to understand the mechanisms of infiltration and evaporation (Moulla, 2005; Farid *et al*., 2015).

5. Results

5.1. General parameters

Table 3 displays the analytical results of groundwater samples collected in this area. Naturaly, groundwater was alkaline (Krishnaraj *et al*., 2011). The pH value of water samples ranges from 7 to 8.6. All the samples are alkaline with average pH value of 7.96. The EC ranges from 483 to 6070(µS/cm) indicating wide variation on these values. This area's high aridity (low precipitation and high evaporation) contributes to high salt concentrations in groundwater (Singh *et al*., 2017; Mallick *et al*., 2018). The highest concentrations of EC (> 2000 µS/cm, W15, W17, W5, W10, W22 and W 27) are situated close to the El Golea Lake formed by evaporitic rock (Guerradi, 2012). Spatial variability shows that this minerali-

zation increases towards the center and in the southern section of the research area (Figure 9).

Wells	pH	Cl^-	NO_3^-	SO_4^{2-}	HCO_3^-	Na^+	K^+	Ca^{2+}	Mg^{2+}	EC (µS/cm)	TDS
W1	7.2	106	0	553	439	168	22	182	52	1694	522
W2	7	129	0	186	525	194	31	59	31	1348	1154
W3	7.3	132	0	397	329	176	33	108.5	45	1544	1221
W4	7.57	243	5.8	497	238	230	57	38.5	100	1894	1409
W5	8	604	0	1008	378	443.5	38	97	276	3920	2859
W6	7.4	121	14	90	335.5	89	12	15	84	870	705
W7	7.8	125	0	250	686	271	18	125	40	1410	1104
W8	7.94	50	12	108	201	41	11.5	47.5	27	517	358
W9	7.95	90	1	278	366	127.5	36	131	50	1100	874
W10	8.24	185	0	718	823.5	340	16	190	100	2440	2100
W11	8.1	115	2	660	497	194	21	172.5	92	1800	1686
W12	8.1	180	1	70	213.5	74	17.5	85	26	685	472
W13	8.6	105	1	300	628	125	24	116	90	1171	820
W14	8.5	55	18	150	506	86	9	94	56	894	670
W15	7.7	650	0	1675	592	745.5	43	265	195	6070	4250
W16	8.3	180	0	450	723	262.5	40	166	79.5	1810	1482
W17	8	725	0	1025	1272	722.5	104.5	271	179	4240	3628
W18	8.3	295	4	387.5	970	452.5	28	177.5	65	1100	874
W19	8.1	105	0	552	440	168	22	183	51.5	1700	1523
W20	8.1	128	0	185	524	194	31	59	34	1350	1155
W21	8.1	130	0	396	329	176	33	108	45	1545	1211
W22	7.8	25	1	456	518.5	182.5	24.5	105	63	2020	1822
W23	8	105	2	158	637.5	202	41.5	87.5	37	1350	966
W24	7.95	170	22	352.5	369	182.5	42.5	120	43.5	1500	990
W25	8.2	210	4	800	351	350	43.5	157.5	49	1630	991
W26	8.1	40	12	110	244	50	10.5	62.5	27	483	339
W27	8.12	580	0	1225	396.5	480.5	32	230	148.5	3350	3200
W28	8.6	70	21	117.5	445	130	11.5	87.5	28.5	780	660

Table 3. Analytical results for the different water points in mg/L.

Tabla 3. Resultados de los análisis de los diferentes puntos acuíferos, en mg/L.

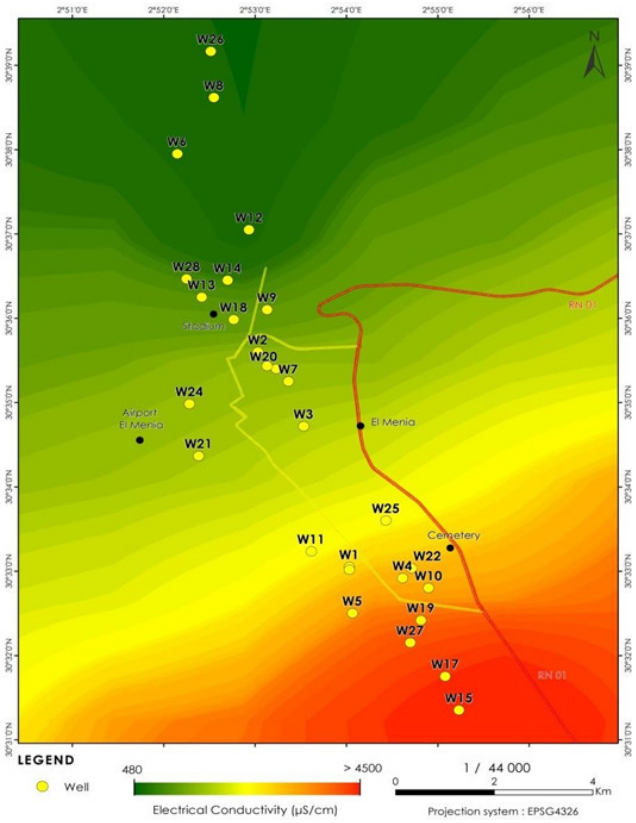

Figure 9. Iso-salinity contour map of the El Golea shallow aquifer.

Figura 9. Mapa de iso-salinidad de lacuífero somero de El Golea.

Based on the concentration of the major cations (Table 2), Na^+ is the most dominant cation ranging from 41 to 480.5 mg/L (mean: 245 mg/L) followed by Ca^{2+} ranging from 15 to 271 mg/L (mean: 126.5 mg/L), Mg^{2+} ranging from 27 to 276 mg/L (mean: 75 mg/L) and K^+ ranging from 9 to 104.5 mg/L (mean: 31 mg/l). HCO3- is the most dominant anion ranging from 201 to 1272 mg/L (mean: 499 mg/L) followed by SO_4^{2-} ranging from 70 to 1675 mg/L (mean: 470 mg/L), Cl^- ranging from 25 to725 mg/L (mean: 202 mg/L) and NO_3^- ranging from 0 to 22 mg/L (mean: 4 mg/L).

The higher concentration of Na^+ in groundwater of this area can be explained by the fact of evaporation process and the weathering of silicate rocks (Rajmohan and Elango, 2004).

The high concentration of Ca^{2+} and Mg^{2+} is responsible for hardness of the groundwater. In this area, the high concentration of Ca^{2+} and Mg^{2+} can indicate the presence of carbonate containing minerals. High HCO_3^- values can also indicate the presence of carbonate containing minerals and/or presence of degraded organic matter in the study area (Rina *et al.*, 2012). The high concentration of SO_4^{2-} in the groundwater in this area might be due to the dissolution of gypsum/anhydrite minerals (Mallick *et al.*, 2018). Close to the lake (W5, W15, W17 and W27), we observed high concentration of Cl^-. It might be due to the leaching of evaporitic rock (Halite) (local effect). Commonly, nitrates concentration greater than 10 mg/L is a result of anthropogenic activities (sewage waste disposal and leakage from septic tanks) (Böhlke, 2002; WHO, 2012). In this area, the high values of nitrates can be attributed to the agricultural practices and/or the presence of leakage from septic tanks.

5.2. Groundwater chemistry and water type

The first approach used to classify the chemical type of water is based on the concentration of various predominant cations and anions (Marghade *et al.*, 2012). For this, the trilinear diagram of Piper (1953) presents a very useful tool in determining chemical relationships in groundwater (Walton, 1970). The plot of chemical analysis on this trilinear diagram is shown in (Figure 10). Regarding cations, most of the samples are mixed-type (64 %), some are sodium type (32 %) and one sample is magnesium type (4%). While for anions, some samples are mixed-type (36%), some are bicarbonate type (36 %), seven samples

are sulphate type, and finally, one sample is chloride type. It's also suggested by Figure 10 that alkaline earth and strong acids exceeded the alkali earths and weak acids in most groundwater samples. The most dominant water types present in this region are mixed Ca-Mg-Cl-SO_4 (14 samples 50%) followed by Ca-HCO_3^- and Na-Cl with five samples (18 %) for both types, and finally, mixed Ca-Na-HCO_3 with four samples (14 %). This suggests that the groundwater hydrochemistry is controlled by water rock interaction and anthropogenic pollution. In the end, Piper diagram shows that groundwater samples are of alkaline-bicarbonate type in the recharge area (W26 and W8), substituting to alkali-mixed type (W20, W2 and W7) along the groundwater flow direction and at last becoming sodium chloride type at the lake of El Golea (W17 and W15).

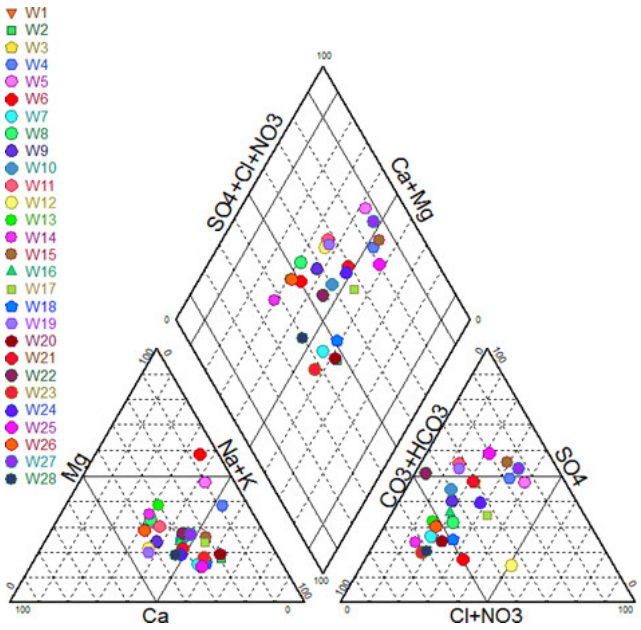

Figure 10. Piper's diagram for the phreatic aquifer.

Figura 10. Diagrama de Piper de las aguas del acuífero freático.

5.3. Statistical analysis

The general statistics of the analyzed parameters are shown in Table 4. A high standard deviation is noticed for all of parameters except pH. It can be explained by the influence of a wide range of hydrochemical factors on the groundwater chemistry (Zaidi et al., 2017). The coefficient of variation, which is the ratio of the standard deviation to the average, was calculated to describe the homogeneity of the series of values reported in Table 2. The results in this table indicate a fairly high coefficient for EC, TDS, K^+, Mg^{2+}, SO_4^{2-}, Na^+ and Cl^-, resulting in low homogeneity. A moderate coefficient of variation is observed for HCO_3^- and Ca^{2+}; the coefficient of variation for pH is quite low, indicating good homogeneity.

	Average	Standard deviation	Variation coefficient (%)
EC(µS/cm)	1793	1237	69
TDS	1430	973	68
pH	7.95	0.4	5
Na^+	245	180	74
K^+	31	19	62
Ca^{2+}	126.5	65.6	52
Mg^{2+}	75	59	79
Cl^-	202	192.6	95.5
SO_4^{2-}	470	387	82
HCO_3^-	499	238	48
NO_3^-	4	7	163

Table 4. Statistical description of the chemical analysis results in mg/L.

Tabla 4. Descripción estadística de los resultados de los análisis químicos, en mg/L.

5.3.1. Application of PCA

The relationship between the number of significant statistics (Rs) and the total number of relationships (Nt) provides some insight about the nature of the statistical distribution (Bougharriou *et al.*, 2018). If this ratio is greater than the value of the significant statistic (Cs), then the statistical distribution of the correlation matrix is good. In this case 0.72 Rs/Nt = 34/66), Cs = 0.24, i.e. 0.72 > 0.24. These results prove that the statistical distribution of the correlation matrix is good.

5.3.2. Correlation matrix

The correlation analysis of groundwater quality parameters suggests the hydrological process controls the evolution of groundwater and its chemical properties (Mallick *et al.*, 2018). The value of R > 0.7 indicates strong correlation, while R value 0.5-0.7 indicates moderate correlation between the variables. A total of 28 groundwater samples from this area were examined. The results of the correlation matrix analysis (Table 5) show a very strong and positive relationship between EC and Cl^-, SO_4^{2-}, Na^+ and Mg^{2+}. A moderate positive relationship is observed between EC and (K^+ and Ca^{2+}) with R equals to 0.57and 0.69, respectively. This high correlation between EC and the majority of chemical elements indicates the contribution of these ions on the conductivity of groundwater. Strong and positive correlation

between Na^+ and Cl^- indicates similar source of these ions. Nitrate is not much significant but positively correlates with pH.

Variables	pH	EC	HCO_3^-	Cl^-	NO_3^-	SO_4^{2-}	Na^+	K^+	Ca^{2+}	Mg^{2+}
pH	1									
EC	-0.12	1								
HCO_3^-	0.21	0.37	1							
Cl^-	-0.02	**0.88**	0.40	1						
NO_3^-	0.22	-0.37	-0.31	-0.3	1					
SO_4^{2-}	-0.04	**0.94**	0.28	**0.84**	-0.37	1				
Na^+	-0.002	**0.89**	**0.62**	**0.91**	-0.33	**0.87**	1			
K^+	-0.12	**0.57**	0.49	**0.66**	-0.23	0.49	**0.67**	1		
Ca^{2+}	0.16	**0.69**	**0.59**	**0.62**	-0.40	**0.78**	**0.77**	0.44	1	
Mg^{2+}	0.01	**0.85**	0.29	**0.86**	-0.28	**0.80**	**0.75**	0.46	0.47	1

Table 5. Correlation matrix for different water points.

Tabla 5. Matriz de correlación de los diferentes puntos de agua.

5.3.3. Correlation circle and individual projection

The application of the PCA on the adopted variables in this table could improve our knowledge on the main factors that determine the mechanism of the mineralization acquisition of all the 28 water samples (individuals).

Examination of the correlation circle drawn on the plane of the factorial axes F1 and F2 shows a good distribution of the parameters studied. The first two axes F1 and F2 express respectively 58.52% and 12.82% of the total variance (Table 6).

Variables	Rotated component matrix	
	Factor1	Factor2
pH	-0.02	**0.88**
Cl^-	**0.92**	-0.056
NO_3^-	**-0.48**	0.3
SO_4^{2-}	**0.91**	-0.11
HCO_3^-	**0.56**	**0.52**
Na^+	**0.96**	0.06
K^+	**0.69**	-0.04
Ca^{2+}	**0.8**	0.28
Mg^{2+}	**0.82**	-0.11
EC	**0.94**	-0.16

Table 6. Principal Component Analysis.

Tabla 6. Análisis de Componentes Principales.

The inertia principal axis F1, in the variables space has a strong positive loading on: EC, SO_4^{2-}, Cl^-, Na^+, K^+, Ca^{2+} and Mg^{2+} (values > 0.75), a moderately positive loading on HCO_3^- (values 0.75–0.50) and a moderately negative loading on NO_3^-. The weights of these parameters are 0.94, 0.91, 0.92, 0.96, 0.69, 0.82 and 0.56, respectively, as shown in the Table 5. Those parameters contributing to more than 55% of the total variance explains why EC has a significant contribution for F1 and indicates the geogenic factors related to dissolution (calcite, halite, and gypsum) and ion exchange. The high loading of EC, SO_4^{2-}, Cl^-, Na^+, K^+, Ca^{2+} and Mg^{2+} indicates mineralization of rocks and soil (Yakubo *et al.*, 2009; Mallick *et al.*, 2018). However, the significant factor loading of NO_3^- in this factor can be attributed to the anthropogenic origin related to the domestic (septic tanks) and agricultural activities in this study area. The second axes F2 represents 13% of the total variance and is highlighted by significant factor loading (> 0.5) of pH and HCO3-. The weight for these parameters is 0.88 and 0.52, respectively. This factor reflects the signature of natural water recharge and water-soil/rock interactions (Freeze and Cherry, 1979; Olobaniyi and Owoyemi, 2006) (Figure 11).

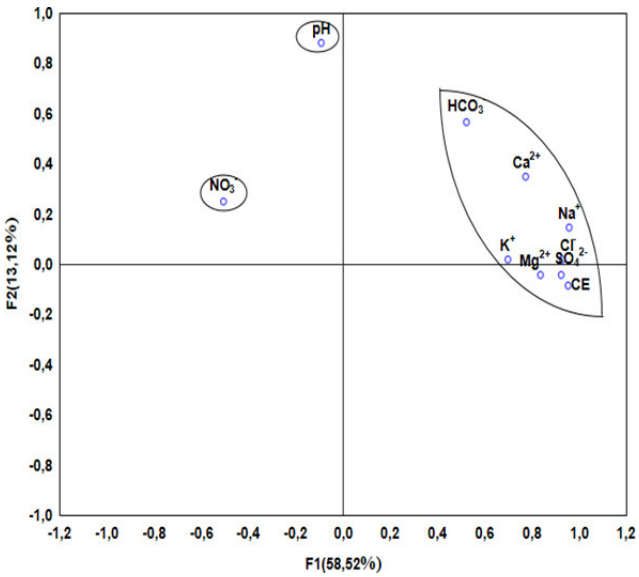

Figure 11. Correlation circles for factors F1-F2.

Figura 11. Círculos de correlación sobre el plano de los factores F1-F2.

5.3.4. Hierarchical Cluster Analysis

The HCA of 28 samples collected and analyzed was performed based on the Ward method and Pearson test. In this case, a dendrogram

(Figure 12) showing two distinct clusters was obtained. The first class shows the relationship between Na^+, Cl^-, Mg^{2+}, SO_4^{2-}, K^+, Ca^{2+}, HCO_3^- and EC. This cluster, similar to that presented for the first component of PCA, could indicate the important role of water-rock interaction in controlling groundwater chemistry. The second class regroups pH and NO_3^-. The parameters of this cluster are similar to the parameters of the first component of PCA and could indicate a relationship between the alkalinity of the samples and bicarbonates.

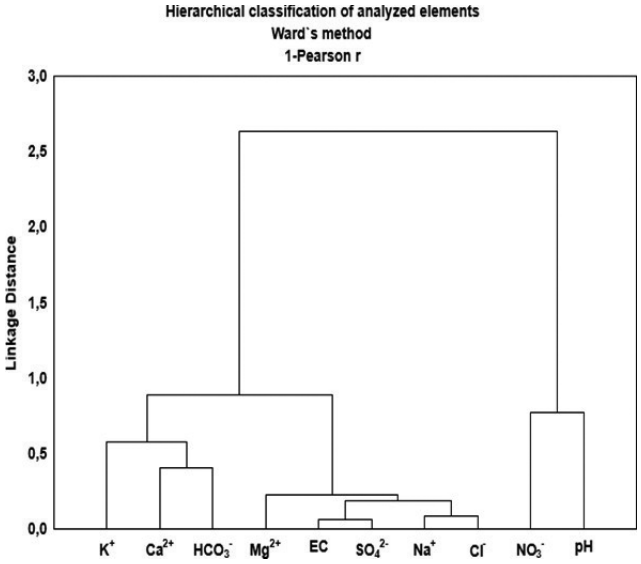

Figure 12. Dendrogram of variables.

Figura 12. Dedrograma de las variables.

5.4. Stable Isotopes

Stable isotopes of the water molecule ($\delta^{18}O$ vs δ^2H) are presented in Table 7. The δ^2H and $\delta^{18}O$ values of the groundwater samples range from -59.5‰ to -46.4‰ and -6.6‰ to -3.5‰. The weighted averages of δ^2H and $\delta^{18}O$ were of -53.15‰ and -5.83‰ vs V-SMOW respectively. Because the low precipitation that characterizes this arid zone (20 mm/year), we have no data about regular measurements of δ^2H and $\delta^{18}O$ in rainfall**.** So**,** due to proximity to study area, the Global Meteoric Water Line (GMWL) $\delta^2H = 8\delta^{18}O + 10$ (2) (Craig, 1961), Sfax's Local Meteoric Lines (LMWL) $\delta^2H = 8\delta^{18}O + 13.5$ (3) defined by Abid *et al.* (2009) and Mean modern rainfall in Sahara ($\delta^{18}O$ = -5.1‰, δ^2H = -26‰) (Edmunds *et al.*, 2003) are presented as a reference for comparison with the groundwater samples of El Golea phreatic aquifer.

Wells	SI CALCITE	SI GYPSUM	SI DOLOMITE	SI HALITE
W1	0.32	-0.46	-0.09	-6.39
W2	-0.03	-1.35	-0.53	-6.21
W3	0.01	-0.79	-0.56	-6.26
W4	-0.61	-1.17	-1	-5.89
W5	-0.12	-0.59	0.03	-5.25
W6	-0.80	-2.23	-1.04	-6.57
W7	0.37	-0.94	0.06	-6.1
W8	-0.47	-1.59	-1.39	-7.27
W9	0.14	-0.86	-0.34	-6.56
W10	0.57	-0.39	0.66	-5.86
W11	0.33	-0.43	0.2	-6.3
W12	-0.22	-1.57	-1.16	-6.47
W13	0.3	-0.9	0.3	-6.51
W14	0.16	-1.24	-0.09	-6.93
W15	0.47	0.02	0.62	-5.02
W16	0.48	-0.61	0.45	-5.97
W17	0.83	-0.17	1.29	-4.98
W18	0.62	-0.68	0.6	-5.53
W19	0.32	-0.46	-0.09	-6.93
W20	-0.03	-1.35	-0.53	-6.21
W21	0.01	-0.79	-0.56	-6.26
W22	0.18	-0.76	-0.06	-6.97
W23	0.22	-1.26	-0.13	-6.29
W24	0.1	-0.80	-0.45	-6.13
W25	0.13	-0.4	-0.44	-5.79
W26	-0.28	-1.48	-1.12	-7.29
W27	0.28	-0.13	0.18	-5.24
W28	0.09	-1.35	-0.5	-6.64

Table 7. $\delta^{18}O$ and δ^2H groundwater contents.

Tabla 7. Contenidos en ^{18}O y δ^2H de las aguas subterráneas.

6. Discussion

6.1. Hydrogeochemical Assesments

6.1.1. Weathering and Dissolution: Ca^{2+}/Mg^{2+}ratio

Calcium and magnesium in groundwater can be the result from different sources, the leaching of limestone, dolomites, gypsum, and also from the cation exchange process. Carbonate rocks react with groundwater in the following two reactions:

$$CaCO_{3(calcite)} + H_2O + CO_2 \rightarrow Ca^{2+} + 2HCO_3^- \quad (4)$$

$$CaMg(CO_3)_{2(dolomite)} + 2H_2O + 2CO_2 \rightarrow Ca^{2+} + Mg^{2+} + 4HCO_3^- \quad (5)$$

By calculating this ratio, we can identify the carbonate mineral responsible for the presence of calcium and magnesium in groundwater samples. If this ration is close to 1, then the dissolution of dolomite is dominant; if this ratio is between 1-2, then the dissolution of calcite is dominant (Mayo and Loucks, 1995). A ratio higher than 2 indicates a non-carbonate origin of these two elements. Figure 13a shows that most of the water samples have a ratio between 1 and 2; indicating that the calcite dissolution is dominant. There are also 7 water samples with a ratio < 1 (W4, W5, W6, W13, W15,

W17 and W27) characterized by the dolomite dissolution, and two water samples with a ratio higher than 2 (W1and W19), which probably indicates ion cation exchange effect (clay minerals).

6.1.2. Weathering and Dissolution: Na^+ vs Cl^-

In semi-arid and arid regions, Na^+ vs Cl^- relationship has often been used to identify the mechanism for acquiring salinity and saline intrusions (Herczeg and Edmunds, 1999). This ratio used also to determine dominant silicate weathering and ion-exchange in groundwater. Figure 13b shows that 14 water samples are close to the 1:1 line (dissolution line), which is characteristic of halite dissolution in groundwater. It is also observed that 6 water samples are above the 1:1 line which is explained by the Na^+ derivate of from silicate weathering reaction and 6 water samples are below the line1:1 indicate evaporation dominance (Jankowski and Acworth, 1997; Singh *et al*., 2017).

6.1.3. Weathering and Dissolution: Ca^{2+}vs HCO_3^-

The influence of evaporate dissolution, silicate weathering or carbonate weathering on groundwater chemistry can be identified by a plot between Ca^{2+} vs HCO_3^- (Singh *et al*., 2017). The scatter plot illustrated in Figure 13c shows that 12 samples are distributed above the 1 :1 equiline, indicating that the carbonate and clay minerals (silicate) weathering contributes to groundwater mineralization (Datta and Tyagi, 1996; Tziritis *et al*., 2017). Moreover, it can be observed that 16 samples are distributes below the 1:1 equiline, reflecting the predominance of evaporate dissolution.

6.1.4. Weathering and Dissolution: Ca^{2+}vs SO_4^{2-}

The plot illustrated in Figure 13d indicates that most of samples trend along and above the 1:1equiline with some samples are close to this equiline, which indicates the presence of dissolution of evaporates rock like gypsum ($CaSO_42H_2O$) or anhydrite ($CaSO_4$) in the area.

However, in the other case where some samples deviate significantly from the 1:1 equiline, the few high individual SO_4^{2-} values may be due to anthropogenic factors such as the use of soil amendments (Tziritis *et al*., 2017) and an augmentation in Ca^{2+} is probably due to reverse ion-exchange (Sheikhy Narany *et al*., 2014).

6.1.5. Ion Exchange

The scattered plot between (Ca^{2+}+Mg^{2+}) and (HCO_3^-+SO_4^{2-}) identifies the ion exchange process. If the samples are close to equiline (1:1 line) so the dominant process in the aquifer is the dissolution of dolomite, calcite or gypsum (Li *et al*., 2014). Ion exchange tends to shift the points right to the 1:1line due to excess of (HCO_3^-+SO_4^{2-}) while the excess of (Ca^{2+}+Mg^{2+}) means that the major process will reverse ion exchange and where the samples tends to shift left to the 1:1 line (Singh *et al*., 2014). The plot of (Ca^{2+}+Mg^{2+}) vs (HCO_3^-+SO_4^{2-}) (Figure 13e) shows that most of samples are close to the equiline line, indicating that dissolution of carbonate minerals (calcite and dolomite), and gypsum are the dominant reactions (Fisher and Mulican, 1997; Mc Lean *et al*., 2000). One sample (W5) has a high concentration of (Ca^{2+}+Mg^{2+}) indicates that reverse ion exchange and carbonate weathering is the most dominant process (Kumar *et al*., 2009; Krishnaraj *et al*., 2011; Rina *et al*., 2013).

6.1.6. Evaporation

The evaporation process is a climatic factor that can increase ions concentrations in groundwater. An effect of evaporation can be ascertained by the use of Na^+ versus Cl^- ratio of groundwater. When this factor is the prevailing process, we show that this ratio (Na^+ versus Cl^-) remains constant with increase in EC (Jankowski and Acworth, 1997). Consequently, the evaporation effect can be observed when the plot of Na/Cl versus EC would give a horizontal line. In our case study, the plot of (Na^+/Cl^-) vs EC of the groundwater samples (Figure 13f) shows that all the samples fall on horizontal trend line, indicating that the evaporation effect is the major process taking place in this area.

6.2. Geochemical modeling

In general, the interaction processes between water and the aquifer matrix controls groundwater geochemistry (Kaur *et al*., 2019). One of the objectives of the saturation index calculation is to predict the mineralogical aspect of the solid matrix of the reservoir rock without the need to collect samples of the latter (Appelo and Postma, 2004; Bouteraa *et al*., 2019). Table 8 summarizes the results of the saturation index calculations for the selected minerals (Calcite, Dolomite, gypsum, and Halite).

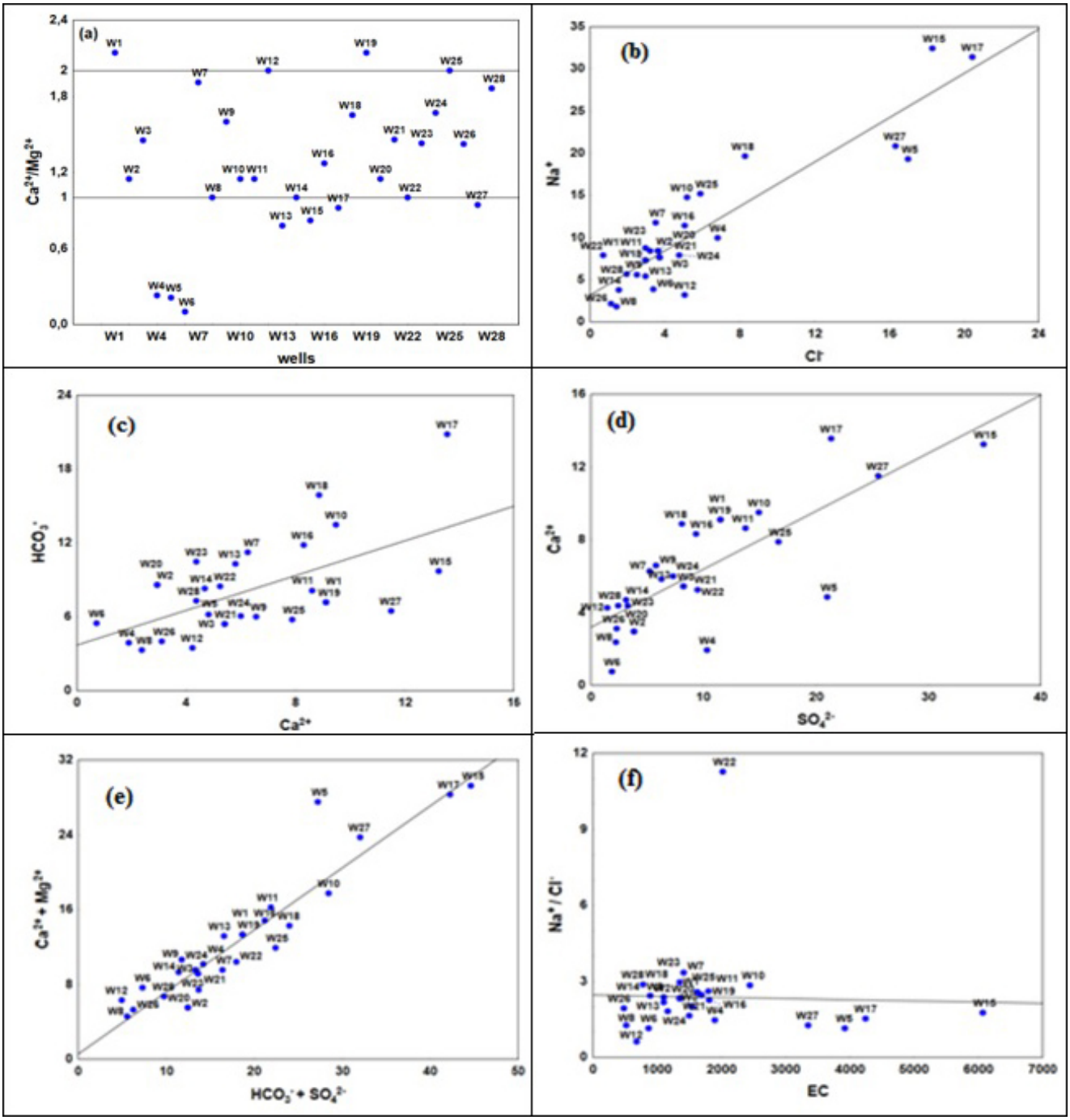

Figure 13. Bivariate plots of a) well numbers vs Ca^{2+}/Mg^{2+}, b) Na^+ vs Cl^-, c) Ca^{2+}vs HCO_3^-, d) Ca^{2+} vs SO_4^{2-}, e) (Ca^{2+}+Mg^{2+}) vs (HCO_3^-+SO_4^{2-}) and f) (Na^+/Cl^-) vs EC.

Figura 13. Representación de a) número de pozo vs Ca^{2+}/Mg^{2+}, b) Na^+ vs Cl^-, c) Ca^{2+} vs HCO_3^-, d) Ca^{2+} vs SO_4^{2-}, e) (Ca^{2+}+Mg^{2+}) vs (HCO_3^- +SO_4^{2-}) y f) (Na^+/Cl^-) vs EC.

Table 8 shows that calcite has positive saturation values in most wells (20 wells), for dolomite, only10 wells have positive saturation values indicating oversaturation with respect to these two minerals and a tendency to precipitate (Figure 14a). For gypsum, all the samples were below the equilibrium state indicating undersaturation with respect to this mineral (Figure 14b). Given the arid climate, this is probably to be a result of evaporation (Gaofeng *et al.*, 2010). For halite, the values are too low, resulting in a fairly low saturation (Figure 14c).

In Figure 15, the δ^2H and $\delta^{18}O$ data of phreatic groundwater samples were plotted on a diagram that relates $\delta^2H = f(\delta^{18}O)$ and compared to the Global Meteoric Water Line (GMWL) (Craig,

		$\delta^{18}O$ (‰)	σ	$\delta^{2}H$ (‰)	σ
Phreatic aquifer	W1	-6.4	0.2	-57.0	1
	W2	-3.5	0.2	-46.5	1.2
	W3	-6.6	0.2	-59.5	1
	W4	-5.7	0.2	-48	0.65
	W5	-6.6	0.2	-56	1.15
	W6	-6.2	0.04	-52	1

Table 8. Evolution of mineral saturation index using PHREEQC.

Tabla 8. Evolución de los índices de saturación de los minerales obtenidos con PHREEQC.

1961), Sfax's Local Meteoric Lines (LMWL) defined by Abid *et al.* (2009) and Mean modern rainfall in Sahara (Edmunds *et al.*, 2003).

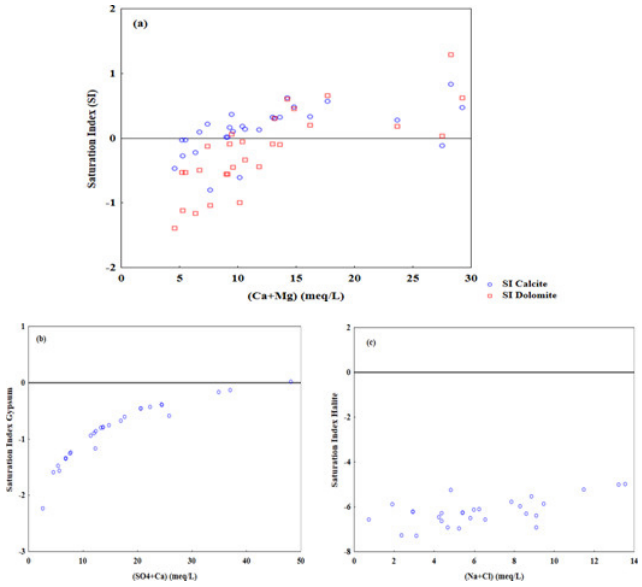

Figure 14. Saturation index variation of a) carbonate minerals, b) gypsum, and c) halite.

Figura 14. Variación del índice de saturación de a) minerales carbonatados, b) yeso, y c) halita.

In this diagram (Figure 14), the scatter plot of phreatic aquifer groundwater follows the trend line $\delta^{2}H = 3.53\delta^{18}O - 32.6$ (6) with $R^2 = 0.65$. we observed that all of the samples were located largely below both the GMWL of Craig (Craig, 1961) and Sfax's local meteoric lines (South Tunisia) defined by Abid *et al.* (2009) indicating their old origin. These depleted values of $\delta^{2}H$ and $\delta^{18}O$ can be explained by the presence of mixes of phreatic groundwater and Continental Intercalaire (CI) waters the main source of irrigation in this region (actually this study area has hundreds of wells of CI aquifer essentially used for irrigation). The most important example of this mixes of groundwater between CI aquifer and phreatic aquifers is the isotopic data of the sample W2 which present values of $\delta^{2}H$ and $\delta^{18}O$ close to isotopic values from CI aquifer (Table 7 and 2). Moreover, Hakimi *et al.* (2021) suggested the existence of mixing of the typical old CI groundwater with younger and evaporated water infiltrated under the dune of the Great Occidental Erg.

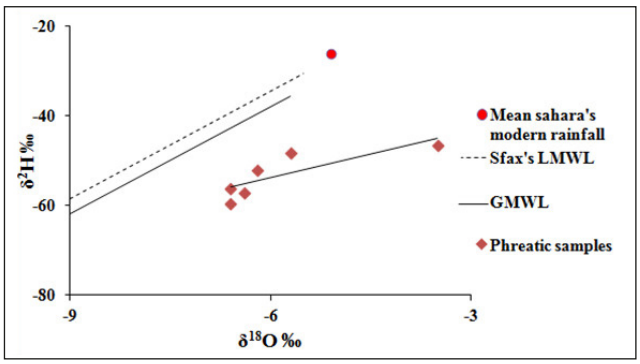

Figure 15. Oxygen18-Deuterium relationship in regional groundwater.

Figura 15. Relación Oxígeno18-Deuterio en las aguas subterráneas de la región.

7. Conclusions

This study is aimed to determine the hydrochemical process of groundwater mineralization in the El Golea oasis, located in Algerian Sahara. The spatial variability of EC shows an increase of this parameter towards the center and the south of the region, the values range from 483 to 6070 (µS/cm) indicating a wide variation. According to Piper's classification, the dominant hydrogeochemical facies of groundwater samples in this area are mixed Ca-Mg-Cl-SO_4 (14 samples 50%), followed by Ca-HCO_3 and Na-Cl with five samples (18 %) for both types, and finally mixed Ca-Na-HCO_3 with four samples (14 %).

Multivariate statistical analysis of the groundwater samples confirmed the predominance of the above-mentioned geogenic and anthropogenic factors. The results of the correlation matrix analysis show a very strong and positive relationship between EC and Cl^-, SO_4^{2-}, Na^+ and Mg^{2+}. A moderate positive relationship is observed between EC and (K^+ and Ca^{2+}) with R equals to 0.57 and 0.69, respectively. This high correlation between EC and the majority of chemical elements indicates the contribution of these ions on the conductivity of groundwater. The application of principal component analysis showed that the first axes F1 has a very strong correlation between EC and the majority of chemical elements, with the

exception of nitrates, which appear to be of anthropogenic origin. The second axes F2 is highlighted by significant factor loading (> 0.5) of pH and HCO_3^- reflecting the signature of natural water recharge and water soil/rock interactions. Hierarchical Cluster Analysis (HCA) showing two distinct clusters were obtained and indicating the important role of water-rock interaction in controlling groundwater chemistry.

The ions ratio of Ca^{2+}/Mg^{2+}, Na^+ vs Cl^-, Ca^{2+} vs HCO_3^-, Ca^{2+} vs SO_4^{2-}, (Ca^{2+} + Mg^{2+}) and (HCO_3^- + SO_4^{2-}) and (Na^+/Cl^-) vs EC shows the importance of weathering, dissolution, ion exchange and evaporation processes on the acquisition of mineralization.

Relation between groundwater level and saturation index of minerals discloses the result of evaporation process on groundwater chemistry. In this arid zone, all groundwater samples are undersaturated with respect to evaporite minerals. On the other hand, carbonate minerals (calcite) are oversaturated in.

Isotopic assessments supplemented the hydrogeochemical and statistical results for groundwater. At the level of the El Golea oasis characterized by an arid climate, the study of ^{18}O and ^{2}H of this shallow aquifer showed that samples groundwater have undergone evaporative fractionation, These depleted values of isotopic composition seem to indicate that this groundwater is composed from mixes of phreatic groundwater and Continental Intercalaire (CI) (old origin) (sample W2).

Acknowledgements

We would like to thank Prof. Antonio Pulido Bosch for his expert advice and encouragement throughout this manuscript.

References

Abid, K., Trabelsi, R., Zouari, K., and Abidi, B. (2009). Caractérisation hydrogéochimique de la nappe du Continental Intercalaire (sud tunisien) / Hydrogeochemical characterization of the Continental Intercalaire aquifer (southern Tunisia). Hydrological Sciences Journal, 54(3), 526–537. https://doi.org/10.1623/hysj.54.3.526.

Aghazadeh, N., Chitsazan, M., and Golestan, Y. (2017). Hydrochemistry and quality assessment of groundwater in the Ardabil area, Iran. Applied Water Science, 7(7), 3599–3616. https://doi.org/10.1007/s13201-016-0498-9.

Alberto, W. D., Valeria, A. M. A., Fabiana, P. S., and Cecilia, H. A. (n.d.). Pattern recognition techniques for the evaluation of spatail and temporal variations in water quality. A case study: Suqui a river basin (Cordoba–Argentina). 14.

Allia, Z., Chebbah, M., and Ouamane, A. (2018). Analyse et evaluation de la qualité des eaux du systéme aquifére Mio-Pliocéne dans le Zab Chergui, bas sahara septentrional. 235-244.

Al-Khashman, O. A., Al-Muhtaseb, A. H., and Ibrahim, K. A. (2011). Date palm (Phoenix dactylifera L.) leaves as biomonitors of atmospheric metal pollution in arid and semi-arid environments. Environmental Pollution, 159(6), 1635–1640. https://doi.org/10.1016/j.envpol.2011.02.045.

Amrani, S., and Hinaje, S. (2014). Hydrodynamisme et minéralisation des eaux souterraines de la nappe phréatique Plio-Quaternaire du plateau Timahdite - Almis Guigou (moyen atlas, Maroc). 16.

Appelo, C. A. J., and Postma, D. (2004). Geochemistry, groundwater and pollution. CRC press.

Belkhiri, L., Boudoukha, A., Mouni, L., and Baouz, T. (2010). Application of multivariate statistical methods and inverse geochemical modeling for characterization of groundwater — A case study: Ain Azel plain (Algeria). Geoderma, 159(3–4), 390–398. https://doi.org/10.1016/j.geoderma.2010.08.016.

Benajiba, M. H., Saoud, Y., Lamribah, A., Ahrikat, M., Amajoud, N., and Ouled-Zian, O. (2013). Évaluation de la qualite microbienne des eaux de la nappe phréatique de Martil au Maroc. Revue des sciences de l'eau, 26(3), 223–233. https://doi.org/10.7202/1018787ar.

Ben Ammar S., Taupin Jean-Denis, Zouari K., Khouatmia M., and Ben Assi, M. (2014). Etude géochimique et isotopique d'un aquifère phréatique côtier anthropisé : nappe de Oussja-Ghar El Melah (Tunisie). In : T. M. Daniell (ed.), Van Lanen H.A.J. (co-ed.), Demuth S. (co-ed.), Laaha G. (co-ed.), Servat Eric (co-ed.), Mahé Gil (co-ed.), Boyer Jean-François (co-ed.), Paturel Jean-Emmanuel (co-ed.), Dezetter Alain (co-ed.), Ruelland D. (co-ed.). Hydrology in a changing world : environmental and human dimensions. Wallingford : AISH, p. 269-275. (Publication - AISH ; 363). Friend-Water 2014 : Hydrology in a Changing World : Environmental and Human Dimensions, 7., Montpellier (FRA), 2014/10/7-10. ISBN 978-1-907161-41-4. ISSN 0144-7815.

Besbes, M., Babasy, M., Kadri, S., Latrech, D., Mamou, A., Pallas, P., and Zammouri, M. (2004). Conceptual framework of the North Western Sahara Aquifer System. Shared Aquifer Resources.

Böhlke, J.-K. (2002). Groundwater recharge and agricultural contamination. Hydrogeology Journal, 10(1), 153–179. https://doi.org/10.1007/s10040-001-0183-3.

Boughariou, E., Bahloul, M., Jmal, I., Allouche, N., Makni, J., Khanfir, H., and Bouri, S. (2018). Hydrochemical and statistical studies of the groundwater salinization combined with MODPATH numerical model: case of the Sfax coastal aquifer, Southeast Tunisia. Arabian Journal of Geosciences, 11(4), 1-13.

Bouteldjaoui, F., Kettab, A., and Bessenasse, M. (2016). Evaluation de la qualité des eaux souterraines par combinaison des méthodes hydrogéochimique, statistiques et géostatistique: Cas de la plaine de Ain Oussera. https://doi.org/10.13140/RG.2.2.18487.68004.

Bouteraa, O., Mebarki, A., Bouaicha, F., Nouaceur, Z., and Laignel, B. (2019). Groundwater quality assessment using multivariate analysis, geostatistical modeling, and water quality index (WQI): A case of study in the Boumerzoug-El Khroub valley of Northeast Algeria. Acta Geochimica, 38(6), 796–814. https://doi.org/10.1007/s11631-019-00329-x.

Busson, G. (1972). Le Mésozoïque saharien .2ème partie : essai de synthèse des données des sondages algéro-tunisiens. Publ. Cent. Rech., Zone arides, CNRS, Paris, ser. Géol., 11 (1 et 2), 810 p.

Castany, G. (1982). Bassin sédimentaire du Sahara septentrional (Algérie-Tunisie)-Aquiféres du Continental Intercalaire et du Complexe Terminal [Sedimentary basin of northern Sahara (Algeria and Tunisia), aquifers of Continental Intercalaire and the Complex Terminal], Bulletin Bureau. Recherches Géologiques Miniéres (BRGM), 3, 127–147.

Coetsiers, M., and Walraevens, K. (2006). Chemical characterization of the Neogene Aquifer, Belgium. Hydrogeology Journal, 14(8), 1556–1568. https://doi.org/10.1007/s10040-006-0053-0.

Cornet, A. (1964). Introduction à l'hydrogéologie saharienne. Géographie Physique et Géologie Dynmaique, 61, 5-72.

Craig, H. (1961). Standard for Reporting Concentrations of Deuterium and Oxygen-18 in Natural Waters. Science, 133(3467), 1833–1834. https://doi.org/10.1126/science.133.3467.1833.

Datta, P. S., and Tyagi, S. K. (1996). Major ion chemistry of groundwater in Delhi area: chemical weathering processes and groundwater flow regime. Journal of Geological Society of India (Online archive from Vol 1 to Vol 78), 47(2), 179-188.

Dubost, D. (1992). Aridité, agriculture et développement: le cas des oasis algériennes. Sécheresse, 3(2), 85-96.

Edmunds, W. M., Guendouz, A. H., Mamou, A., Moulla, A., Shand, P., and Zouari, K. (2003). Groundwater evolution in the Continental Intercalaire aquifer of southern Algeria and Tunisia: Trace element and isotopic indicators. Applied Geochemistry, 18(6), 805–822. https://doi.org/10.1016/S0883-2927(02)00189-0.

El-Yamine, G., Yassine, N., Choayb, B., Ettayib, B., Soumia, H., and Moussa, H. (2018). Breeding ecology of the common coot (Fulica atra) at El-Golea Lake (Algerian Sahara). 4.

Farid, I., Zouari, K., Rigane, A., and Beji, R. (2015). Origin of the groundwater salinity and geochemical processes in detrital and carbonate aquifers: Case of Chougafiya basin (Central Tunisia). Journal of Hydrology, 530, 508–532. https://doi.org/10.1016/j.jhydrol.2015.10.009.

Farnham, I. M., Johannesson, K. H., Singh, A. K., Hodge, V. F., and Stetzenbach, K. J. (2003). Factor analytical approaches for evaluating groundwater trace element chemistry data. Analytica Chimica Acta, 490(1–2), 123–138. https://doi.org/10.1016/S0003-2670(03)00350-7.

FIDA (2016). L'avantage des terres arides. Rome, Italie. 40 pp.

Freeze, R. A., Cherry, J. A. (1979). Groundwater. Prentice-Hall, inc, New-Jersey. 604 pp.

Gaofeng, Z., Yonghong, S., Chunlin, H., Qi, F., and Zhiguang, L. (2010). Hydrogeochemical processes in the groundwater environment of Heihe River Basin, northwest China. Environmental Earth Sciences, 60(1), 139–153. https://doi.org/10.1007/s12665-009-0175-5.

Garrels, R. M., and Mackenzie, F.T. (1967). Origin of the Chemical Compositions of Some Springs and Lakes. Equilibrium Concepts in Natural Water Systems, 222–242. DOI: 10.1021/ba-1967-0067.ch010.

Gouaidia, L., and Laouar, M. (2018). Origine de la mineralisation des eaux souterraines d 'un aquifere dans une zone semi - aride, cas de la nappe de la merdja, nord - est algerien. International Journal of Environment and Water, 6(2), 104–118.

Gouskov N, and Cornet, A. (1952). The waters of the Lower Cretaceous Continental in the Algerian Sahara (known Albian Nappe). XIX Cong. Geol. Inter. geology and water problems in Algeria. Volume II. Data on Hydrogeology Algeria.

Guendouz, A. (1985). Contribution à l'étude géochimique et isotopique des nappes profondes du Sahara Nort-Est septentrional, Algérie. Thése de doctorat 3éme cycle. Univ. Paris-Sud. Orsay, p. 243.

Guerradi, H. (2012). Etude géochimique et minéralogique du lac d'El Menia, thése magister université ouargla.

Hacĕne, H., Rafa, F., Chebhouni, N., Boutaiba, S., Bhatnagar, T., Baratti, J. C., and Ollivier, B. (2004). Biodiversity of prokaryotic microflora in El Golea Salt lake, Algerian Sahara. Journal of Arid Environments, 58(3), 273–284. https://doi.org/10.1016/j.jaridenv.2003.08.006.

Hakimi, Y., Orban, P., Deschamps, P., and Brouyere, S. (2021). Hydrochemical and isotopic characteristics of groundwater in the Continental Intercalaire aquifer system: Insights from Mzab Ridge and surrounding regions, North of the Algerian Sahara.

Journal of Hydrology: Regional Studies, 34, 100791. https://doi.org/10.1016/j.ejrh.2021.100791.

Hamed, Y., Ahmadi, R., Hadji, R., Mokadem, N., Dhia, H. B., and Ali, W. (2014). Groundwater evolution of the Continental Intercalaire aquifer of Southern Tunisia and a part of Southern Algeria: Use of geochemical and isotopic indicators. Desalination and Water Treatment, 52(10–12), 1990–1996. https://doi.org/10.1080/19443994.2013.806221.

Herczeg, A. L., Edmunds, W. M. (2000). Inorganic ions as tracers. In Environmental tracers in subsurface hydrology (pp. 31-77). Springer, Boston, MA.

Jankowski, J., and Acworth, R. I. (1997). Impact of debris-flow deposits on hydrogeochemical processes and the developement of dryland salinity in the Yass River Catchment, New South Wales, Australia. Hydrogeology Journal, 5(4), 71-88.

Kabour, A., and Chebbah, L. (2017). Caractérisation hydro-chimique et mise à jour de la salinité des eaux souterraines en région aride: cas de l'aquifère du grès carbonifère de Kénadsa (Sud-Ouest Algérien). Géo-Eco-Trop, 41(1), 99-106.

Karimipour, F., Delavar, M. R., and Rezayan, H. (2005). Neighborhood analysis in water pollution estimation. Environmental Informatics Archives, 3, 232-238.

Kaur, L., Rishi, M. S., Sharma, S., Sharma, B., Lata, R., and Singh, G. (2019). Hydrogeochemical characterization of groundwater in alluvial plains of River Yamuna in Northern India: an insight of controlling processes. Journal of King Saud University-Science, 31(4), 1245-1253.

Kendra, P. L., Blumenfeld, S., and Lu, C. (2010). Eau potable, biodiversité et développement. Edited by CBD. Montréal. Available at: https://www.cbd.int/development/doc/cbd-good-practice-guide- water-booklet-web-fr.pdf.

Kloppmann, W., Bourhane, A., Schomburgk, S., and Asfirane, F. (2011). Salinisation des masses d'eaux en France: du constat au diagnostic. work document, BRGM, Aout, Orléans.

Knouz, N., Boudhar, A., Bachaoui, E. M., and Aghzaf, B. (2016). Étude de la vulnérabilité des nappes à la pollution en zones semi-arides: cas de la nappe phréatique des Béni Amir au Maroc. Méditerranée. Revue Géographique des Pays Méditerranéens/ Journal of Mediterranean Geography.

Krishnaraj, S., Murugesan, V., Sabarathinam, K. V., Paluchamy, C., and Ramachandran, A. (2011). Use of hydrochemistry and stable isotopes as tools for groundwater evolution and contamination investigations. Geosciences, 1(1), 16–25.

Kumar, M., Kumari, K., Singh, U. K., and Ramanathan, A. L. (2009). Hydrogeochemical processes in the groundwater environment of Muktsar, Punjab: conventional graphical and multivariate statistical approach. Environmental Geology, 57(4), 873-884.

Li, P., Qian, H., Wu, J., Zhang, Y., and Zhang, H. (2013). Major ion chemistry of shallow groundwater in the Dongsheng Coalfield, Ordos Basin, China. Mine Water and the Environment, 32(3), 195-206.

Li, P., Wu, J., Qian, H., Lyu, X., and Liu, H. (2014). Origin and assessment of groundwater pollution and associated health risk: a case study in an industrial park, northwest China. Environmental Geochemistry and Health, 36(4), 693-712.

Mallick, J., Singh, C. K., AlMesfer, M. K., Kumar, A., Khan, R. A., Islam, S., and Rahman, A. (2018). Hydro-geochemical assessment of groundwater quality in Aseer Region, Saudi Arabia. Water, 10(12), 1847.

Marghade, D., Malpe, D. B., and Zade, A. B. (2012). Major ion chemistry of shallow groundwater of a fast growing city of Central India. Environmental Monitoring and Assessment, 184(4), 2405-2418.

Mayo, A. L., and Loucks, M. D. (1995). Solute and isotopic geochemistry and ground water flow in the central Wasatch Range, Utah. Journal of Hydrology, 172(1-4), 31-59.

Melouah, O., and Zerrouki, H. (2020). Hydrochemical study of sources salinity in shallow water springs of northern algerian Sahara. Journal of Fundamental and Applied Sciences, 12(1), 291-317.

Ministry of the Environment (2002). L'eau. La vie. L'avenir. Québec. 94 pp.

Mortimore, M., Anderson, S., Cotula, L., Davies, J., Faccer, K., Hesse, C., *et al*. (2009). Dryland Opportunies: A new paradigm for people, ecosystems and development. International Union for Conservation of Nature (IUCN).

Moulla, A. (2005). Colloque International. Les Ressources en Eau Souterraine au Sahara . Algérie. 1–37 pp.

Moulla, A., Guendouz, A., Cherchali, M., Chaid, Z., and Ouarezki, S. (2012). Updated geochemical and isotopic data from the Continental Intercalaire aquifer in the Great Occidental Erg sub-basin (south-western Algeria). Quaternary International, 257, 64-73.

Nascimento, J. (2017). Gestion intégrée de l'eau et développement durable. Le cas du Cap-Vert. Thése de doctorat, Université de Rouen, France, 557 pp.

Observatoire Régionale de l'Environnement (2015). L'environnement en Poitou-Charentes, France, 388 pp.

Olobaniyi, S. B., and Owoyemi, F. B. (2006). Characterization by factor analysis of the chemical facies of groundwater in the deltaic plain sands aquifer of Warri, western Niger delta, Nigeria. African Journal of Science and Technology, 7(1), 73-81.

Olsen, R. L., Chappell, R. W., and Loftis, J. C. (2012). Water quality sample collection, data treatment and results presentation for principal components analysis–literature review and Illinois River watershed case study. Water research, 46(9), 3110-3122.

Parkhurst, D. L., and Appelo, C. A. J. (1999). User's guide to PHREEQC, ver. 2. A computer program for speciation, batch-reaction, one-dimensional transport, and inverse geochemical calculations. Investigations Report 99-4259. US Geological Survey Water-Resources.

Paul, L. C., Suman, A. A., and Sultan, N. (2013). Methodological analysis of principal component analysis (PCA) method. International Journal of Computational Engineering & Management, 16(2), 32-38.

Pazand, K., Khosravi, D., Ghaderi, M. R., and Rezvanianzadeh, M. R. (2018). Identification of the hydrogeochemical processes and assessment of groundwater in a semi-arid region using major ion chemistry: A case study of Ardestan basin in Central Iran. Groundwater for Sustainable Development, 6, 245-254.

Penna, D., Stenni, B., Šanda, M., Wrede, S., Bogaard, T. A., Gobbi, A., and Chárová, Z. (2010). On the reproducibility and repeatability of laser absorption spectroscopy measurements for δ^2H and $\delta^{18}O$ isotopic analysis. Hydrology and Earth System Sciences, 14(8), 1551-1566.

Pereira, H. G., Renca, S., and Saraiva, J. (2003). A case study on geochemical anomaly identification through principal components analysis supplementary projection. Applied Geochemistry, 18(1), 37- 44.

Peron, A. (1883). Essai d'une description géologique de l'Algérie. 200 pp.

Piper, A. M. (1953). Agraphical procedure in the geochemical interpretation of water analysis. Transactions of the American Geophysical Union, 25, 914–928.

Raj, D., and Shaji, E. (2017). Fluoride contamination in groundwater resources of Alleppey, southern India. Geoscience Frontiers, 8(1), 117-124.

Rajmohan, N., and Elango, L. J. E. G. (2004). Identification and evolution of hydrogeochemical processes in the groundwater environment in an area of the Palar and Cheyyar River Basins, Southern India. Environmental Geology, 46(1), 47-61.

Rina, K., Datta, P. S., Singh, C. K., and Mukherjee, S. (2012). Characterization and evaluation of processes governing the groundwater quality in parts of the Sabarmati basin, Gujarat using hydrochemistry integrated with GIS. Hydrological Processes, 26(10), 1538-1551.

Rina, K., Singh, C. K., Datta, P. S., Singh, N., and Mukherjee, S. (2013). Geochemical modelling, ionic ratio and GIS based mapping of groundwater salinity and assessment of governing processes in Northern Gujarat, India. Environmental Earth Sciences, 69(7), 2377-2391.

Saadé-Sbeih, M., and Jaubert, R. (2012). L'exploitation des eaux souterraines en Syrie centrale: rupture rhétorique et continuité des pratiques. Méditerranée. Revue géographique des pays méditerranéens / Journal of Mediterranean Geography, 119, 73-81.

Salman, A. S., Zaidi, F. K., and Hussein, M. T. (2015). Evaluation of groundwater quality in northern Saudi Arabia using multivariate analysis and stochastic statistics. Environmental Earth Sciences, 74(12), 7769-7782.

Sappa, G., Ergul, S., and Ferranti, F. (2014). Geochemical modeling and multivariate statistical evaluation of trace elements in arsenic contaminated groundwater systems of Viterbo Area,(Central Italy). SpringerPlus, 3(1), 1-19.

Sheikhy Narany, T. S., Ramli, M. F., Aris, A. Z., Sulaiman, W. N. A., and Fakharian, K. (2014). Spatiotemporal variation of groundwater quality using integrated multivariate statistical and geostatistical approaches in Amol–Babol Plain, Iran. Environmental monitoring and assessment, 186(9), 5797-5815.

Singh, C. K., Kumari, R., Singh, R. P., Shashtri, S., Kamal, V., and Mukherjee, S. (2011). Geochemical evidences of high fluoride concentration in groundwater of Pokhran, area of Rajasthan, India. 2011. Bull. Env. Contam. Toxicol, 86(2), 152–158.

Singh, C. K., Rina, K., Singh, R. P., and Mukherjee, S. (2014). Geochemical characterization and heavy metal contamination of groundwater in Satluj River Basin. Environmental earth sciences, 71(1), 201-216.

Singh, C. K., Kumar, A., Shashtri, S., Kumar, A., Kumar, P., and Mallick, J. (2017). Multivariate statistical analysis and geochemical modeling for geochemical assessment of groundwater of Delhi, India. Journal of Geochemical Exploration, 175, 59-71.

Rao, N. S., Rao, P. S., and Varma, D. D. (2013). Spatial variations of groundwater vulnerability using cluster analysis. Journal of the Geological Society of India, 81(5), 685-697.

Rao, N. S., and Chaudhary, M. (2019). Hydrogeochemical processes regulating the spatial distribution of groundwater contamination, using pollution index of groundwater (PIG) and hierarchical cluster analysis (HCA): a case study. Groundwater for Sustainable Development, 9, 100238.

Subramani, T., Rajmohan, N., and Elango, L. (2010). Groundwater geochemistry and identification of hydrogeochemical processes in a hard rock region, Southern India. Environmental monitoring and assessment, 162(1), 123-137.

Tziritis, E., Skordas, K., and Kelepertsis, A. (2016). The use of hydrogeochemical analyses and multivariate statistics for the characterization of groundwater resources in a complex aquifer system. A case study in Amyros River basin, Thessaly, central Greece. Environmental Earth Sciences, 75(4), 339.

Tziritis, E. P., Datta, P. S., and Barzegar, R. (2017). Characterization and assessment of groundwater resources in a complex hydrological basin of central

Greece (Kopaida basin) with the joint use of hydrogeochemical analysis, multivariate statistics and stable isotopes. Aquatic Geochemistry, 23(4), 271-298.

UNESCO (ERESS) (1972). Etude des Ressources en Eau au Sahara Septentrional. United Nations Educational Scientific and Cultural Organization, Paris. Rapport final.

Varol, M., Gökot, B., Bekleyen, A., and Şen, B. (2012). Spatial and temporal variations in surface water quality of the dam reservoirs in the Tigris River basin, Turkey. Catena, 92, 11-21.

Voutsis, N., Kelepertzis, E., Tziritis, E., and Kelepertsis, A. (2015). Assessing the hydrogeochemistry of groundwaters in ophiolite areas of Euboea Island, Greece, using multivariate statistical methods. Journal of Geochemical Exploration, 159, 79-92.

Walton, W. C. (1970). Groundwater resources evaluation. New York: McGraw-Hill.

World Health Organization (WHO) (2012). Directives de qualité pour l'eau de boisson quatrième édition intégrant le premier additif, Journal of Chemical Information and Modeling. DOI: 10.1080/02626669609491505.

Yakubo, B., Yidana, S. M., and Nti, E. (2009). Hydrochemical analysis of groundwater using multivariate statistical methods—The Volta region, Ghana. KSCE Journal of Civil Engineering, 13(1), 55–63. https://doi.org/10.1007/s12205-009-0055-2.

Yang, C., Yanguo, T., Yuanzheng, Z., Wei, W., Xiaosi, S., and Yang, L. (2011). Hydrogeochemical evolution of groundwater in the lake area of northern ordos cretaceous basin. In: 2011 International Symposium on Water Resource and Environmental Protection (Vol. 1, pp. 153-156). IEEE.

Yang, Q., Wang, L., Ma, H., Yu, K., and Martín, J. D. (2016). Hydrochemical characterization and pollution sources identification of groundwater in Salawusu aquifer system of Ordos Basin, China. Environmental Pollution, 216, 340-349.

Zaidi, F. K., Al-Bassam, A. M., Kassem, O. M., Alfaifi, H. J., and Alhumidan, S. M. (2017). Factors influencing the major ion chemistry in the Tihama coastal plain of southern Saudi Arabia: evidences from hydrochemical facies analyses and ionic relationships. Environmental Earth Sciences, 76(14), 1-16.

Zeddouri, A., Derradji, F., and Hadj-Saïd, S. (2010). Salinity origin of terminal complex water in Ouargla region (south east of Algeria). Phys. Chem. News, 53, 62-69.